Investigation on High-Power-Density Design of Small PM Motors Focusing on Air Gap Configuration

Kazuaki Usami, Toshihiko Noguchi (Shizuoka University,Japan)

Abstract. This paper describes a case study of high-power-density design of small permanent magnet (PM) motors focusing on their air gap configurations. Two types of the PM motors, i.e., a radial air gap type and an axial air gap type, are comparatively discussed. Comparison between the two types has been conducted from the viewpoints of I-T characteristics, N-T characteristics, efficiency maps, torque ripple characteristics, and so forth. It has been clarified that the axial air gap type has significant advantages to achieve the high-power-density under some limited conditions.Start

1. Introduction

Electrification of various equipment such as automotives, industrial machines, home appliances, etc. is intensively promoted to improve the energy conversion efficiency and the control performance. Electrical motors play an important role for the electrification, and improvement of their efficiency and power density is an unavoidable issue to expand their application fields. Permanent magnet synchronous motors (PMSMs) have recently been employed instead of induction motors because of their higher efficiency and higher power density. In the case of pan-cake shaped motors, axial air gap PM motors have significant advantages for the improvement of the power density, compared with radial air gap PM motors. In general, when the motors are designed to have a flat pan-cake proportion, higher-power-density design can be achieved because the rotor surface area generating the electromagnetic torque of the axial air gap PM motors is much larger than that of the radial air gap PM motors. In addition, the axial air gap PM motor can easily reduce the copper loss of the windings because of their higher space factor of the stator slots, which is another advantage over the radial air gap PM motor. In the paper, a comparative case study is conducted between a newly developed axial air gap PM motor and an existing benchmark radial air gap PM motor, where both motors are designed to have almost same current-to-torque (I-T) characteristics. A finite element method (FEM) based three-dimensional electromagnetic analyses are carried out to investigate the effectiveness of the axial air gap configuration for the downsizing of the motor.

2. Motor design conditions and three-dimensional electromagnetic analysis

2.1. Motor Design Conditions and Constraints

The following conditions are given in designing the motors:
(1) using same material PM and same volume PM,
(2) setting almost same winding resistance per phase,
(3) assuming the same space factor of the windings, and
(4) using the magnetic material of which iron loss is almost same.
An electromagnetic analysis is conducted with JMAG-Designer 17.1™ to investigate how high the power density of the axial air gap PM motor can be achieved, compared with the radial air gap PM motor.

2.2. Overview of Designed Motors

Figure 1 shows overviews of the designed PM motors and their major dimensions. The radial air gap PM motor is a surface PM (SPM) type of which stator has concentrated windings. Supposing this radial air gap SPM motor as a benchmark, the axial air gap PM motor is designed so that the I-T characteristics of the both motors are identical as described later. The diameter of the axial air gap PM motor is adjusted to make its I-T characteristic equal to that of the radial air gap PM motor.

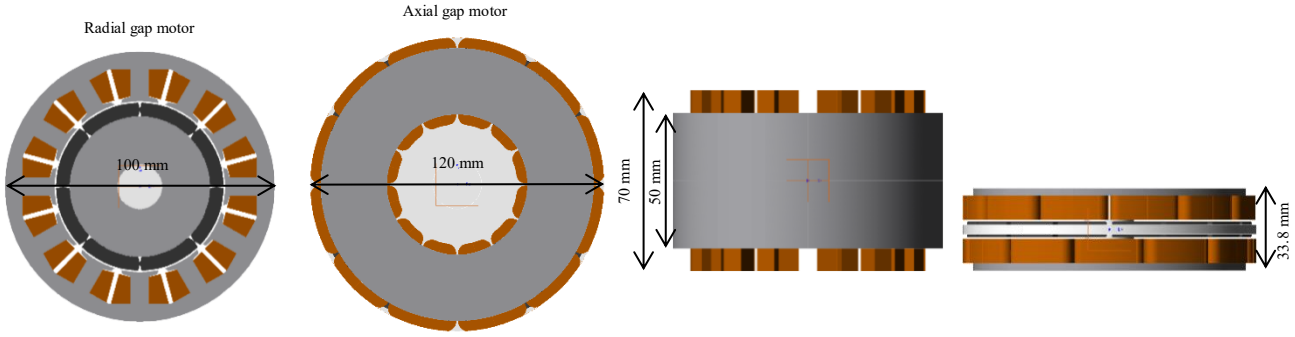

Fig. 1. Overview of designed motors.

2.3. Motor Specifications and Materials Used in Motors

Table 1. Materials used in designed motors.

	Radial gap motor	Axial gap motor
Stator core	35JN440	Somaloy 1000 SP
Rotor core	35JN440	SUS304
Magnet	MNF12E	MNF12E
Shaft	S45C	S45C

Table 2. Specifications of designed motors.

	Radial gap motor	Axial gap motor
Motor type	SPM motor	SPM motor
Outer diameter	Φ100 mm	Φ120 mm
Air gap distance	0.637 mm	0.750 mm
Slot combination	12s8p	24s16p
Coil space factor	40 %	40 %
Number of turns	30 T/slot	26 T/slot
Conductor diameter	Φ1.02 mm	Φ1.03 mm
Phase resistance	0.364 Ω/phase	0.353 Ω/phase
Coil connection	Star connection	Star connection
Current density ($10A_{rms}$/phase)	6.14 A_{rms}/mm^2	6.02 A_{rms}/mm^2
Ld	2.01 mH	0.567 mH
Lq	2.05 mH	0.585 mH

Table 3. Motor dimensions.

	Radial gap motor	Axial gap motor
Outer diameter	Φ100 mm	Φ120 mm
Iron core axial length	50 mm	33.8 mm
Axial length Including coil ends	70 mm	33.8 mm
Iron core volume	392 cm^3	382 cm^3
Volume including coil ends	550 cm^3	382 cm^3

Table 4. Estimated weights of components and whole motors.

	Radial gap motor	Axial gap motor
Stator core	1117 g	868 g
Rotor core	697 g	130 g
Permanent magnet	223 g	223 g
Shaft	122 g	80 g
Windings	394 g	469 g
Total	2554 g	1771 g

Table 1 indicates major specifications of the two motors. The air gap of the axial type is slightly wider than that of the radial type because it is rather difficult to maintain the air gap precisely in the manufacturing process and the attractive axial force in the air gap is remarkably strong. The slot combinations of the both motors are 2:3 based and the number of winding turns of the axial type is chosen 26 to achieve equal I-T characteristic to the radial type. Because the space factors of the windings are identical, the winding resistance of each phase can be almost same by using the same diameter conductors. Therefore, the current densities of the windings are also approximately 6 A for both motors. The inductances are calculated from the electromagnetic analysis results, and it can be found that the inductances of the axial type are approximately quarter of those of the radial type because of the low-winding-turns and the wide air gap.

Table 2 shows materials used in each motor. Soft magnetic composite (SMC) (Somaloy 1000 SP: 220kW/m3) is employed as a stator core material in the axial air gap PM motor because its iron loss at 400 Hz and 1 T is relatively close to that of the electromagnetic steel plate used in the radial air gap PM

motor (35JN440: 178 kW/m3). The rotor cores of the two motors are composed of the electromagnetic steel plates (35JN440) in the radial type and the stainless steel (SUS304) in the axial type, respectively. The axial air gap PM motor employs a non-magnetic material such as SUS304 in the rotor back yoke to prevent the eddy currents. However, a general metal material (S45C) is used for the shaft from a mechanical strength reason.

2.4. Proportions and Dimensions of Designed Motors

Table 3 shows major dimensions of the two motors. As described above, the outer diameter of the axial air gap PM motor is designed to be 20-% larger than that of the radial air gap PM motor in order to make the I-T characteristics equal. The motor axial length of the axial type can be reduced to approximately 68 % of the radial type, and can be reduced down to less than 50 % if the coil ends of the radial type are included. As can be found in the table, the iron core volumes their selves are almost same with each other, but the total volume of the axial type can significantly be reduced when the coil ends of the radial type are included in the motor volume. The volume of the motor cannot always be reduced if the axial air gap configuration is employed due to the limitation of the rotor diameter and its mechanical strength. However, the axial air gap approach is remarkably effective to improve the power density for small motors from 1 to 2-kW output power range.

Table 4 shows estimated weights of the components and the total of each motor. Every weight is calculated from the component volume and the specific gravity. The rotor weight of the axial type is much lower than that of the radial type, which implies that higher power rate is expected. As described previously, both of the motors have the same weight PMs on the rotor, but the total weights of the rotors are very different because of volume difference of the rotor cores. However, the weight of the windings in the axial type is heavier because more slots are in the stator core, which makes the total amount of the conductors higher. The winding weight of the axial type is increased by 19 %, compared with that of the radial type. All in all, however, overall weight of the axial type can be remarkably reduced by 31 %; hence the axial air gap approach is efficient to improve the weight as well as the volume.

3. Operating conditions and operation characteristics of design motors

3.1. Operating Conditions

(1) No-Load electromotive force (e.m.f.)

The motors are operated at 3000 r/min with open windings, and no-load e.m.f. is observed at the motor terminals.

(2) I-T characteristics

Only the q-axis current is given to the motors, and phase angle advancing control is not applied to the motors when the I-T characteristic is examined. The current waveforms are sinusoidal of which effective value is from 0 to 10 A. The rotating speed is kept constant at 3000 r/min throughout the I-T characteristic test.

(3) Rotating speed and Torque (N-T) characteristics

The sinusoidal currents are given to the motors, where the maximum value is 10 A. No voltage drop caused in the inverter and the wire harness is not considered. The inverter DC-bus voltage is fixed at 100 V.

(4) Efficiency maps

The efficiency maps are obtained along with the N-T characteristics described above, so the every condition is exactly same as that of N-T characteristic test. Particularly, a conductor eddy current loss is not taken into account.

(5)Torque waveforms

The torque waveforms are observed under the same conditions as those of the I-T characteristics. In addition, the cogging torque waveforms are obtained by rotating the motors at 60 r/min.

3.2. No-Load Electromotive Force

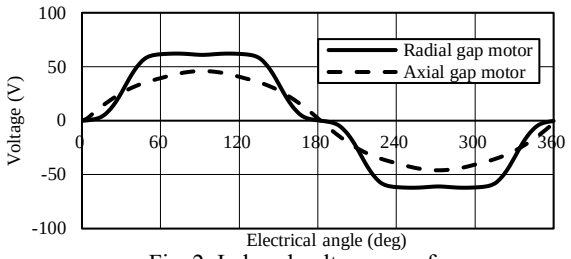

Fig. 2. Induced voltage waveforms.

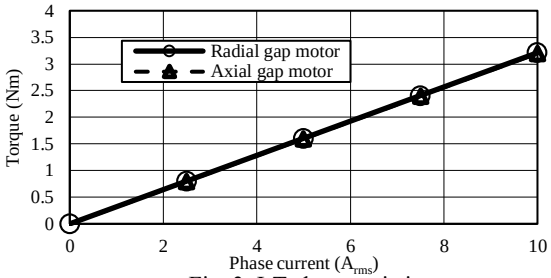

Fig. 3. I-T characreristics.

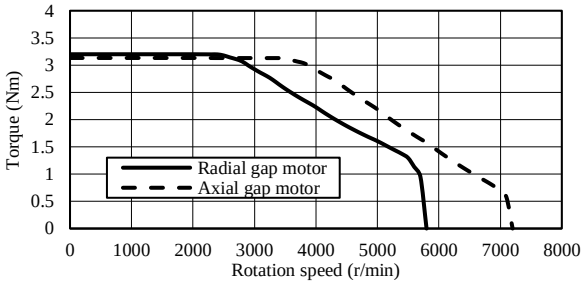

Fig. 4. N-T characteristics.

Figure 2 shows e.m.f. waveforms of the two motors at no load condition. The e,m.f. amplitude of the radial type is approximately 60 V, while that of the axial type is 46 V. The e.m.f. constant of the axial type is lower than that of the radial type, which contributes to the higher-speed operation. In addition, the e.m.f. waveform of axial type is very close to sinusoidal, compared with that of the radial type. Owing to the sinusoidal e.m.f., reduction of the torque ripple is expected by giving the sinusoidal currents to the motor unless the space harmonics of the concentrated winding stator affect the torque generation.

3.3. I-T Characteristics

Figure 3 shows the I-T characteristics of both motors. As can be seen in the figure, the I-T characteristics of the two motors are identical and are linear to the motor current, which implies that magnetic saturation is not occurred in the motors.

3.4. N-T characteristics

Figure 4 shows the N-T characteristics of both motors, where the axial air gap PM motor is capable to rotate in the higher-speed range whereas the torque constant operation region is almost same. As described above, the axial type is capable to operate in the higher-speed range owing to less e.m.f.

3.5. Efficiency Maps

Efficiency maps are indicated in Figs. 5 and 6. The axial type has a larger region where higher efficiency is obtained. However, this large high-efficiency area may slightly be degraded by the conductor eddy current that has not been considered in the analysis. This conductor eddy current loss may be caused because of the fully open slot configuration is introduced to the axial type. It should be noted that there is a highest efficiency area over 95 % in the efficiency map of the axial type.
Figures 7 and 8 shows iron-loss maps, and Figs. 9 and 10 shows copper-loss maps, respectively. The range of the iron-loss variation is from 0 to 10 W, but the copper-losses increase to 100 W in the N-T characteristics; hence both of the motors can be regarded as copper machines. The magnetic materials used in the stator cores, i.e., 35JN440 and Somaloy 1000 SP, play an important role to reduce the iron-losses. In other words, the copper-losses must be suppressed to achieve higher efficiency in these motors. The copper-losses can be reduced by increasing the space factor of the windings, e.g., using flat square windings, or by enlarging the slot area.

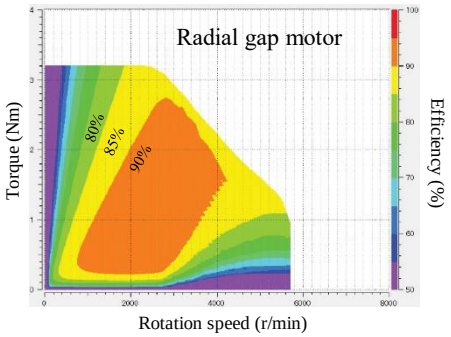

Fig. 5. Efficiency map of radial air gap PM motor.

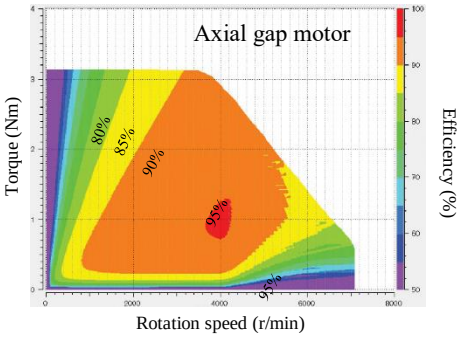

Fig. 6. Efficiency map of axial air gap PM motor.

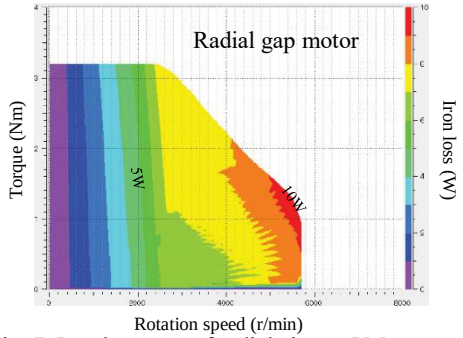

Fig. 7. Iron loss map of radial air gap PM motor.

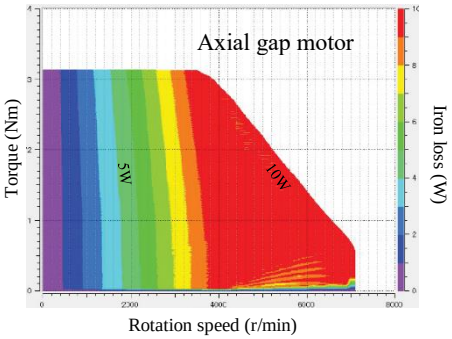

Fig. 8. Iron loss map of axial air gap PM motor.

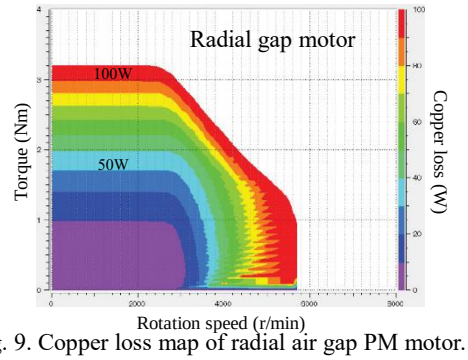

Fig. 9. Copper loss map of radial air gap PM motor.

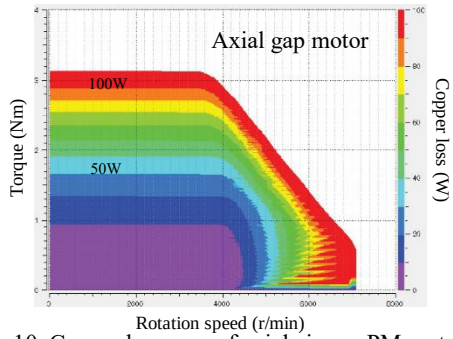

Fig. 10. Copper loss map of axial air gap PM motor.

3.6. Torque Waveforms

Figure 11 shows the torque waveforms of the two motors in the steady state. Both of the motors generate the same average torque, but the torque ripples of the axial type and the radial type are 19.5 % and 14.5 %, respectively. As illustrated in Fig. 1, the double stators of the axial type are skewed, so the torque ripple can effectively suppressed, compared with the radial type. It is considered that the torque ripples are caused by the fifth and the seventh components of the space harmonics, which is mainly generated by the concentrated winding configuration.

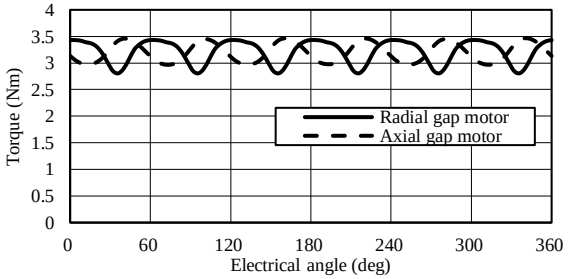

Fig. 11. Torque waveforms.

Figure 12 shows an enlarged one period of the cogging torque waveforms. The peak to peak values of the cogging torque waveforms are 0.42 Nm for the radial type and 0.45 Nm for the axial type, respectively. Compared with the rated average torque, the cogging torque is small enough for many kinds of applications. The torque ripple is varied with the average torque value as shown in Fig. 13.

The torque ripple ratio is almost inverse proportional to the average torque for both motors. It is confirmed that the axial type is slightly superior to the radial type in the higher torque region.

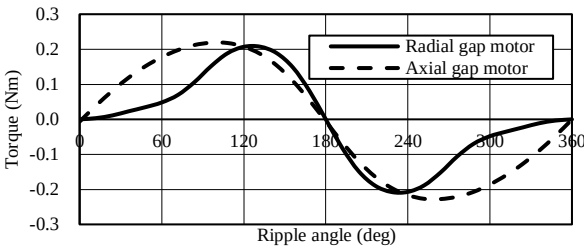

Fig. 12. Cogging torque waveforms.

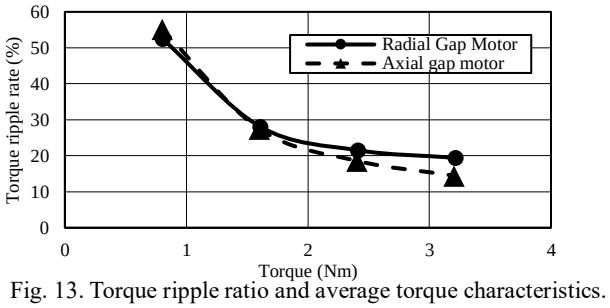

Fig. 13. Torque ripple ratio and average torque characteristics.

4. CONCLUSION

The paper has described a case study of a motor design, where the two types of the motors have been designed, i.e., a radial air gap PM motor and an axial air gap PM motor. Under the same conditions, e.g., the same amount of the PM, the same space factor of the windings, the similar iron-loss property material, and the same winding resistance, it has been found that the axial air gap PM motor can reduce the motor volume (including the coil ends) by 30 % and the motor weight by 30 %, respectively. From another point of view, the axial length of the axial type can be reduced to almost half of the radial type although the diameter is increased by 20 %. In general, the axial air gap PM motor is very suitable for the pan-cake design of the motor because the center space of the double stators can be utilized for the mechanism such as a bearing. In the investigation described in the paper, both motors have employed the same amount of ferrite PMs, but the motor size can further be reduced by taking advantage of Nd bonded PM instead of the ferrite. As a result, overall performance of the axial air gap PM motor has been found to be superior to that of the radial air gap PM motor. However, it is indispensable to enhance the mechanical strength of the axial type rotor because the atrractive force between the stator theeth and the rotor PM poles is significantly strong regardless of the thin rotor stracture. In addition, reduction of the torque ripple is another problem to be solved, which is the future work of this study.

References

[1] H.Kamiyama, T.Noguchi, A.Hattori, Y.Yamada, S.Yokoyama:“Development of High-Torque Density Pancake Motor for Automotive Applications”,IEEJ Annual National Conference (2017)

[2] K.Takishima, K.Sakai:”Starting Characteristics of Axial and Radial Type Ultra-Lightweight Motors Based on Magnetic Resonance Coupling”,IEEJ J. Industry Applications, vol. 8, no. 3, pp. 471-479 (2019)

[3] S. Morimoto, Y. Asano, T. Kosaka, and Y. Enomoto, “Recent Technical Trands in PMSM”, in Proc. IPEC-2014, pp.1997-2003 (2014)

[4] J.A. Tapia, F. Leonardi, and T.A. Lipo: “Consequent-pole Permanent- Magnet Machine with Extended Field-Weakening Capability”, *IEEE Trans. on IA*., Vol. 39, No. 39, pp. 1704-1709 (2003)

[5] M.Aoyama, T.Noguchi,:”Preliminary Experimental Verification of Self-Excited Wound-Field Synchronous Reactive Power for Robust Maximum Torque Per Ampere Control”,ICIT2015 (2015)